Appl. Phys. B 49, 99–108 (1989)

Applied Physics B Photophysics and Laser Chemistry

Quantum-Limited FM-Spectroscopy with a Lead-Salt Diode Laser

A Comparison of Theoretical and Experimental Data

P. Werle[1], F. Slemr[1], M. Gehrtz[2], and C. Bräuchle[3]

[1] Fraunhofer-Institute for Atmospheric Environment Research, Kreuzeckbahnstrasse 19, D-8100 Garmisch-Partenkirchen, Fed. Rep. Germany
[2] IBM Germany, Plant Mainz Laboratories, P.O. Box 2540, D-6500 Mainz, Fed. Rep. Germany
[3] Institute for Physical Chemistry, Sophienstrasse 11, D-8000 München, Fed. Rep. Germany

Received 10 February 1989/Accepted 7 April 1989

Abstract. Ultrasensitive absorption spectroscopy of NO_2 was performed with a tunable lead-salt diode laser (TDL) using a single-tone high-frequency modulation (FM) technique. With a detection bandwidth of 200 kHz, an optical density of 2.7×10^{-5} was detectable at SNR of 1. The detectable optical density could be further improved by reducing the detection bandwidth in agreement with the $\sqrt{\Delta f}$ relationship, reaching 2.5×10^{-6} at a detection bandwidth of 1.56 kHz. Normalized to 1 Hz bandwidth, the demonstrated performance would then correspond to a detectable optical density of 5.9×10^{-8}. This detection limit agrees well with the calculated "quantum limited" performance based on the measured laser power, modulation index, noise figure of the electronic components, and other parameters of the apparatus. These measurements and calculations show that by implementation of the FM technique, the sensitivity of the present TDL absorption spectrometers (TDLAS) can be improved by at least a factor of 10 and possibly even of 100. Such a sensitivity improvement would greatly extend the applicability of TDLAS for trace gas analysis, especially in atmospheric monitoring.

PACS: 07.65

Tunable diode laser absorption spectroscopy (TDLAS) has become a powerful technique for trace gas analysis in industrial and environmental applications [1, 2]. It is technique of choice wherever there is a need for sensitive, highly specific, or rapid measurements of trace gases. In atmospheric science, TDLAS has been used for the measurement of NO, NO_2, N_2O, HNO_3, H_2O, H_2O_2, H_2CO, CO, CH_4, SO_2, HCl, and HF. Potentially, most small molecules can be measured, provided that they possess resolved Doppler broadened rotation-vibration spectra in the wavelength region between 3 and 30 μm [3], and that the sensitivity of TDLAS is sufficient for the given application.

Essentially, two techniques have been applied to achieve the highest TDLAS sensitivity: averaging of fast scans over an absorption line [4, 5], and harmonic ("derivative") detection techniques [6–8]. Both techniques use low frequency modulation of the laser wavelength of the order of several kHz. The best performance of such TDLAS instruments in terms of sensitivity at a detection bandwidth estimated from published data, is indicated in Table 1. Since some of the listed papers lack a clear definition of the detection bandwidth and the detection limit, the detectable optical density at SNR (signal to noise ratio) of 1 may be in error by a factor of 6. Despite this uncertainty, the data illustrate the state of the art.

Table 1. Optical density detectable at a SNR of 1, and estimated detection bandwidth for derivative and fast scan techniques using lead-salt diode lasers

Author	Technique	Det. limit	Δf	Ref.
Schiff et al.	2f, scanning	1×10^{-5}	0.33 Hz	[2]
Cassidy and Reid	avg. fast scan	1×10^{-5}	3.2 Hz	[4]
Silver and Stanton	avg. fast scan	1×10^{-3}	1.56 kHz	[5]
Sachse et al.	2f, w/o scanning	4.5×10^{-5}	3 Hz	[6]
Fried et al.	2f, scanning	1×10^{-5}	1 Hz	[7]
Reid et al.	2f, scanning	6.4×10^{-6}	0.12 Hz	[8]

The two techniques have achieved comparable detection limits corresponding to a detectable optical density of about 1×10^{-5} with a detection bandwidth of 1 Hz. In terms of mixing ratios, such detectable optical density corresponds to detection limits of tenths of ppbv (1 ppbv $= 1 \times 10^{-9}$ volume fraction) for strongly and moderately absorbing molecules when multi-reflection cells with path lengths on the order of 100 m are employed. Weakly absorbing species or species with still lower mixing ratios could not be measured, although there are many applications where such measurements are highly desirable.

Fundamentally, the ultimate detectable optical density of each absorption technique is limited by the photon statistics, i.e. it cannot be better than $\sqrt{n}/n$, where n is the number of photons incident at the ideal detector. Taking into account the power emitted by the commercially available lead-salt diode lasers and the quantum efficiency of the common HgCdTe detectors, the performance of the TDL absorption spectrometers is much worse than the performance limited by the fundamental signal shot noise. Our analysis of the noise frequency spectrum of a lead-salt diode laser [9] and noise measurements on other lasers [10], suggests that $1/f$ noise is responsible for the poor performance of the present TDLAS techniques using low frequency modulation schemes. The noise analysis also indicated that a shot noise ("quantum") limited performance could possibly be achieved with a high frequency-modulation (FM) technique. The purpose of this paper is to demonstrate this possibility.

The paper will report on the ultrasensitive absorption spectroscopy of NO_2 by a single tone FM technique with a *MBE* lead-salt diode laser. In the first section of the paper we briefly review the principles of the FM technique and present a detailed formal description which will be used in the calculation of the FM sensitivity needed for comparison with the measured one. The second section reports on the experimental determination of the FM sensitivity when measuring low partial pressures of NO_2. In the third section, the measured sensitivity is compared with that calculated. The quite good agreement of the measured and calculated signal to noise ratios indicates that the sensitivity achieved corresponds to the "quantum" limited performance. Finally, our results are summarized and presented as points in a sensitivity versus bandwidth domain. This presentation allows an easy comparison of our FM-TDLAS performance with the performance of conventional TDLAS spectroscopy and with some recent FM results.

1. FM Spectroscopy

The use of the FM technique [11] in combination with semiconductor diode lasers is particularly attractive, since these lasers can be directly frequency modulated by the laser injection current [12–14] without using less efficient and expensive external modulators. The laser carrier frequency is modulated directly with a discrete rf frequency added to the laser current by a bias T. The rf energy is transferred into sidebands, and instead of a single emission line the frequency spectrum of the laser output consists of several equally spaced sidebands at integer multiples of the modulation frequency around the carrier. The amplitude distribution of the sidebands depends on the FM modulation index β, which is a measure of the power available in the sidebands. A formal description of the FM signals can be derived from the expression for the electrical laser field

$$E(t) = E_0[1 + M \cdot \sin(\omega_{rf} t + \psi)] \times \exp[i(\omega_c t + \beta \cdot \sin \omega_{rf} t)], \quad (1)$$

where the exponent describes the frequency modulation of the carrier ω_c with frequency ω_{rf} and FM modulation index β. The pre-exponential factor takes into account the influence of the amplitude modulation index M. Equation (1) can be more conveniently expressed as

$$E(t) = E_0(t) \sum_{n=-\infty}^{+\infty} r_n \exp(in\omega_{rf} t) \quad (2)$$

with

$$E_0(t) = E_0 \exp(i\omega_c t)$$

and

$$r_n = r_n(\beta, M, \psi) = \sum_{k=-1}^{+1} a_k J_{n-k}(\beta)$$

$$a_0 = 1; \quad a_{\pm 1} = \pm M/2\mathrm{i}\, \exp(\pm \mathrm{i}\psi).$$

Taking into account the sideband absorptions δ_n and phase shifts ϕ_n at harmonics of the modulation frequency $n\omega_{rf}$ with $n=0, \pm 1, \pm 2, \ldots$ (2) can be transformed into

$$E(t) = E_0(t) \sum_{n=-\infty}^{+\infty} r_n(\beta, M, \psi) \times \exp(\mathrm{i}n\omega_{rf}t) \exp(-\delta_n - \mathrm{i}\phi_n) \quad (3)$$

with $\omega_n = \omega_c + n\omega_{rf}$. In this transformation, the notation of Bjorklund for δ_n, ϕ_n for an assumed Lorentzian lineshape is used [15]:

$$\delta_n = \delta(\omega_n) = \delta_{peak}/[1 + R(\omega_n)^2], \quad (3a)$$

$$\phi_n = \phi(\omega_n) = \delta_{peak} R(\omega_n)/[1 + R(\omega_n)^2], \quad (3b)$$

$$R(\omega_n) = (\Omega - \omega_n)/\Gamma_{1/2}; \quad \delta_{peak} = \alpha L/2, \quad (3c)$$

where R is the sideband detuning from the molecular center frequency Ω and $\Gamma_{1/2}$ is the line half width at half maximum (HWHM). The term αL corresponds to the optical density of the investigated gas with Beer's law peak absorption coefficient α and an absorber pathlength of L. Assuming a square law detector response the electric field $E(t)$ gives rise to a detector current $i_{rf}(t)$ according to:

$$i_{rf}(t) = i_0 \sum_{n,n'=-\infty}^{+\infty} r_n r_{n'}^* \times \exp[\mathrm{i}(n-n')\omega_{rf}t - \delta_n - \delta_{n'} - \mathrm{i}\phi_n + \mathrm{i}\phi_{n'}]. \quad (4)$$

Narrow band detection and demodulation at the modulation frequency ω_{rf} limits the allowed values for n for demodulation to $n' = n \pm 1$:

$$i_{rf}(t) = i_0 Z \exp(\mathrm{i}\omega_{rf}t) + i_0 Z^* \exp(-\mathrm{i}\omega_{rf}t),$$
$$Z = \sum_{n=-\infty}^{+\infty} r_n r_{n+1}^* \exp(-\delta_n - \delta_{n+1} - \mathrm{i}\phi_n + \mathrm{i}\phi_{n+1}). \quad (5)$$

Using $A = 2\,\mathrm{Re}\{Z\}$ (quadrature) and $D = -2\,\mathrm{Im}\{Z\}$ (in phase), the final equation for the interesting frequency components at ω_{rf} at the mixer input port can be written as:

$$i_{rf}(t) = i_0 A(\beta, M, \psi)\cos(\omega_{rf}t) + i_0 D(\beta, M, \psi)\sin(\omega_{rf}t). \quad (6)$$

The above equation is valid for arbitrary frequency modulation index β, amplitude modulation index M and AM/FM phaseshift ψ. The full expressions for the in phase and quadrature components of the signal at any AM/FM phaseshift are quite cumbersome but it is useful to analyze the particular case of an AM/FM phaseshift of $\psi = \pi/2$. The reason for this will become obvious later. The coefficients then reduce to:

$$A(\beta, M, \pi/2) = 2 \sum_{n=-\infty}^{+\infty} (J_{n+1}J_n + K_n) \times \exp(-\delta_{n+1} - \delta_n)\cos(\phi_{n+1} - \phi_n), \quad (7a)$$

$$D(\beta, M, \pi/2) = 2 \sum_{n=-\infty}^{+\infty} (J_{n+1}J_n + K_n) \times \exp(-\delta_{n+1} - \delta_n)\sin(\phi_{n+1} - \phi_n), \quad (7b)$$

$$K_n = M/2(J_nJ_n + J_{n+1}J_{n+1} + J_nJ_{n+2} + J_{n-1}J_{n+1}) + (M/2)^2(J_{n-1}J_n + J_{n+1}J_{n+2} + J_{n-1}J_{n+2} + J_{n+1}J_n). \quad (7c)$$

In the absence of any absorption $\phi_{n+1} - \phi_n \approx 0$ and $-\delta_{n+1} - \delta_n \approx -2\delta'$, where δ' is the broadband background absorption. This yields $D \approx 0$ and $A \approx \Sigma K_n$, using the symmetry characteristics of the Bessel functions, $J_{-n}(\beta) = (-1)^n J_n(\beta)$. The term K_n describes the residual amplitude modulation (RAM) which always accompanys the pure frequency modulation when a semiconductor diode laser is directly modulated by the injection current. The FM/AM index ratio is a laser intrinsic parameter and depends on the laser structure [16]. The RAM manifests itself as a constant signal offset. The phase sensitive detection of the in-phase signal component $D(\beta, M, \pi/2)$ will have a zero baseline, while the quadrature component $A(\beta, M, \pi/2)$ will have an offset proportional to the amplitude modulation. With a local oscillator signal at the mixer LO port proportional to $\sin(\omega_{rf}t + \Theta)$, it is possible to select either the quadrature or the in-phase signal component at the low pass filtered mixer IF output by appropriate adjustment of the detection phase Θ:

$$i_{IF}(t) \approx A(\beta, M, \psi)\cos\Theta + D(\beta, M, \psi)\sin\Theta. \quad (8)$$

RAM-zeroing by proper adjustment of the phase sensitive detection circuitry ($\Theta = \pi/2$) is an effective method to prevent the PMPA input from being overloaded under high amplification conditions during sensitive measurements.

To obtain insight into these relations it is useful to analyze the limit of low absorption and phaseshift [$\exp(-\delta_{n+1} - \delta_n) \approx 1 - \delta_{n+1} - \delta_n$; $\sin(\phi_{n+1} - \phi_n) \approx (\phi_{n+1} - \phi_n)$; $\cos(\phi_{n+1} - \phi_n) \approx 1$; $\delta_n \ll 1$; $\phi_n \ll 1$] under low modulation conditions $\beta < 1$, $M \ll \beta$ with $J_0(\beta) = 1$ and $J_{\pm 1}(\beta) = \beta/2$ while higher order Bessel functions can be neglected and the sums (7a, b) are limited to values of $n = -1$ and $n = 0$. Equation (6) can then be rewritten in the following form:

$$i(t) = i_0(\beta \cdot \Delta\delta \cos\omega_{rf}t + \beta \cdot \Delta\phi \sin\omega_{rf}t), \quad (9)$$

$$\Delta\delta = \delta_{-1} - \delta_1, \quad (9a)$$

$$\Delta\phi = \phi_1 + \phi_{-1} - 2\phi_0, \quad (9b)$$

where the expressions for δ_n and ϕ_n are given by (3), $\Delta\delta$ is the difference in absorption experienced by the upper and lower sideband, and $\Delta\phi$ is the difference between twice the carrier phaseshift and the sum of the sideband phase shift.

2. Experimental Results

The absorption spectroscopy of NO_2 was made with a FM-TDLAS instrument designed for field monitoring of trace gases in the atmosphere. A detailed description of the instrument will be given elsewhere. The measurements were made with the basic experimental setup shown in Fig. 1. A MBE lead-salt diode laser (Fraunhofer-Institute for Metrology, Freiburg) was mounted in a liquid nitrogen cooled dewar and driven by a current from a power supply (modified Laser Control Module, SP 5820, Spectra Physics). The rf-power was generated by a rf-oscillator (SMG, Rohde and Schwarz), attenuated by an adjustable rf-attenuator and coupled into the laser via a bias T. The laser beam was collimated by a 15 mm diameter 90° off-axis paraboloid mirror, passed through a 30 cm sample cell with variable NO_2 partial pressure, and was finally focussed by another 90° off-axis paraboloid mirror onto a photovoltaic HgCdTe detector with a cutoff frequency of 200 MHz (Societe Anonyme de Telecommunications, Paris). The detector element had a diameter of 0.5 mm and was cooled by liquid nitrogen. The detector was biased for optimum signal to noise ratio at the required response frequency of 100 to 120 MHz.

The rf beat signal measured by the detector was amplified by 60 dB, filtered by a high pass filter and fed into a double balanced rf-mixer input. The local oscillator input of the rf-mixer obtained the rf-power from the rf-generator after the rf phase angle had been adjusted with a variable phase shifter. The output of the rf-mixer was amplified by another 40 dB by a post-mixer preamplifier (PMPA) and filtered by an adjustable bandwidth filter (Krohn-Hite 3550). The resulting signal was digitized, stored on a digital oscilloscope (Tektronix 2430A), and transferred via an IEEE interface into a computer.

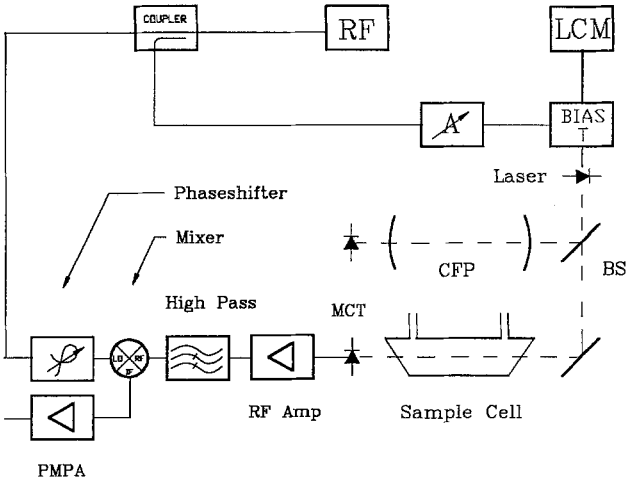

Fig. 1. Basic experimental FM setup

The first and most important prerequisite for sensitive FM spectroscopy is a single mode laser emission with power output as high as possible. Therefore, the laser mode structure was characterized by a 1/4 m grating monochromator (Jarrell Ash) as a function of driving current and operating temperature. Apart from the near-threshold region around 240 mA at 85 K, a narrow single mode emission region was found at a driving current of 950 mA and a temperature of 95 K. Under these conditions the laser emitted at 6.25 μm coinciding with several absorption lines of NO_2. The laser power incident on the HgCdTe detector after passing through the absorption cell was determined by a pyroelectric detector with internal calibration (RS 5900, Laser Precision) and was found to be 1450 μW. This value agreed within a few percent with the signal obtained by the HgCdTe detector when the spectral sensitivity specified by the manufacturer was taken into account. With this incident power the signal noise of the HgCdTe photovoltaic detector at frequencies above 100 MHz was proportional to the square root of the laser power ($\sim\sqrt{P}$), indicating that the signal shot noise dominated other noise sources [9].

The emission spectrum of the laser with the modulation sidebands was observed directly using a scanning confocal Fabry-Perot interferometer (Burleigh, Finesse 125, FSR 3 GHz). The spectra, observed with increasing modulation indices, are shown in Fig. 2, and they display two notable features. The observed linewidth of the laser emission was limited by the resolution of the Fabry-Perot etalon and found to be around 30 MHz. The emission broadening due to the high frequency noise in the laser current supply must have been smaller than that, thus the condition of resolved sidebands was fulfilled. Another notable feature is the almost identical amplitude of the sidebands, indicating extremely low amplitude modulation. A pronounced contribution of AM to the FM would otherwise manifest itself as an obvious asymmetry in the amplitude of the sidebands. From the observed small asymmetry of the sideband amplitudes, the ratio of FM/AM modulation indices M/β can be derived to be less than 0.01. Such a low ratio of FM/AM modulation indices is a prerequisite for high sensitivity FM absorption measurements [17, 20].

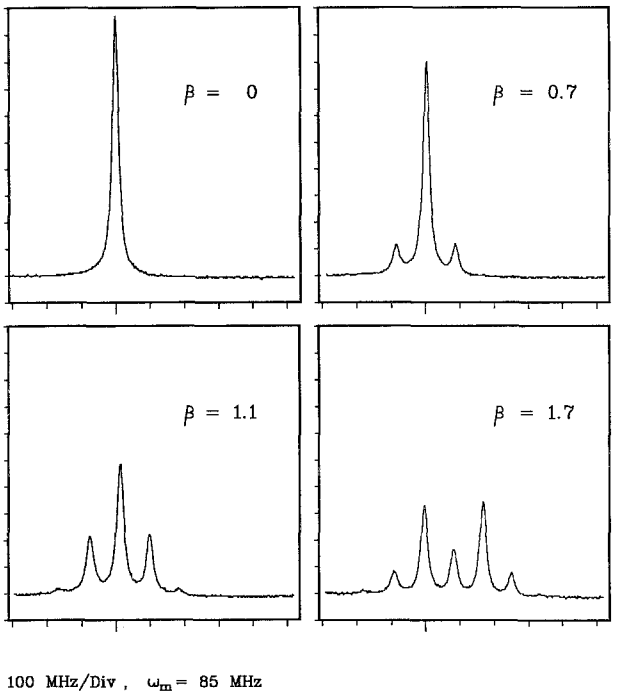

Fig. 2. Spectra of the diode laser emission modulated with increasing rf-power. The spectra were recorded with a scanning Fabry-Perot interferometer

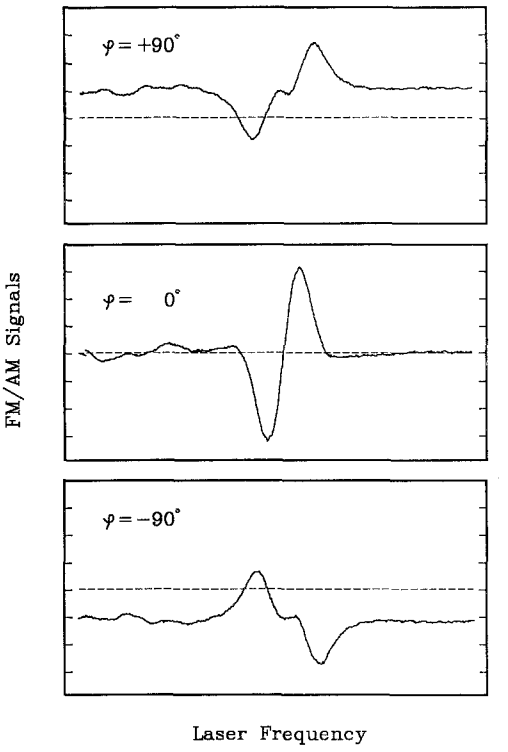

Fig. 3. Appropriate selection of the detection phase allows RAM nulling and the detection of in phase or quadrature signals

The frequency modulation index β can be determined directly from the carrier to side band amplitude ratio, as displayed in the Fabry-Perot spectra in Fig. 2. This procedure requires a careful adjustment of the Fabry-Perot interferometer and is impractical for everyday use. Therefore, a simpler indirect procedure has been tested and compared with the direct determination. In this procedure the laser was scanned over the NO_2 absorption line and the optical density was observed directly with the frequency modulation off and on. The amplitude ratio of the measured optical densities with the frequency modulation on and off equals the ratio of the Bessel functions, $J_0^2(\beta)/J_0^2(\beta=0)$, and from this the modulation index β can be estimated. The direct determination of β by the Fabry-Perot interferometer and the indirect determihation agreed within a few percent.

The FM absorption spectrum of NO_2 was recorded by tuning the laser over the absorption line with a small current ramp superimposed on the laser driving current. Depending on the adjusted phase angle, the resulting spectrum is a mixture of an absorption and dispersion spectrum. Figure 3 shows three scanning spectra of a NO_2 absorption line taken with different phase angles between the optical and the local oscillator signals. In the middle spectrum, the phase angle was adjusted to minimize the RAM-induced signal offset. This optimum phase angle adjustment was designated as Θ^0. The top and the bottom spectra were taken with phase angles changed by $\pm 90°$. The RAM-induced zero offset reached maximum values at $\pm 90°$ phase angle, indicating a phase shift ψ of $\pi/2$ between the amplitude and frequency modulation. This result agrees well with the AM-FM phase shift measured on GaAlAs diode lasers [18, 19], and is also consistent with the measurement on lead-salt diode lasers of Gehrtz et al. [14]. The absence of a sloping background indicates that the phase shift between the amplitude and the frequency modulation does not change substantially with the scanning of the laser frequency over at least 4 linewidths. Even scans over several absorption lines did not show a significant change in FM signal lineshape with our laser. The same result have been obtained with a *BH* laser by Silver and Stanton [20]. These findings differ from the observation by Cooper and Warren [17], who reported a significant change of the phase shift between the AM and FM when scanning a mesa stripe laser. This phase change would prevent an effective zeroing of the signal offset by the phase angle adjustment, and it contributed strongly to the conclusion by Cooper et al. [17] that the single tone FM technique is inferior to the two tone technique.

To demonstrate "quantum limited" performance, the modulation index β was adjusted for a maximum FM signal amplitude to $\beta = 1.1$, which agrees well with

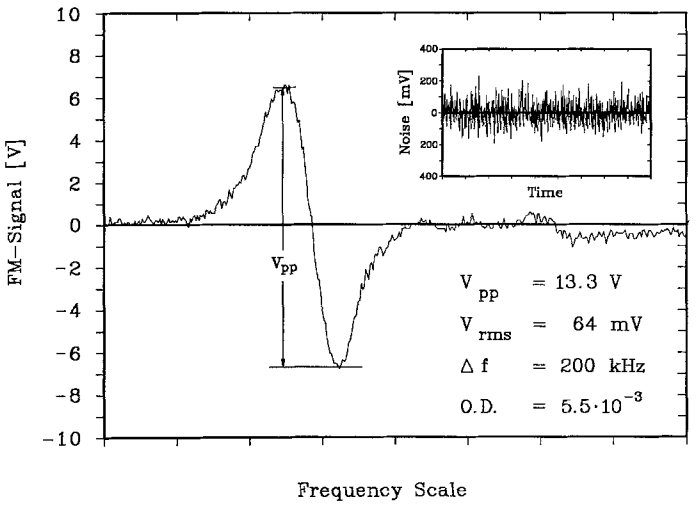

Fig. 4. FM signal at 200 kHz detection bandwidth corresponding to an optical density of 5.5×10^{-3}. The chart with expanded y-axis on the top corner shows the measured noise in the signal

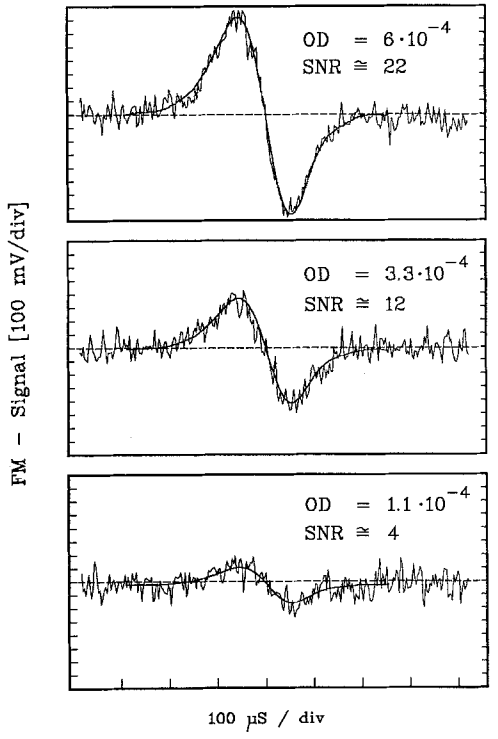

Fig. 5. Same signal as Fig. 4 but successive reduction of the optical density and signal to noise ratio SNR by evacuating the sample cell

calculated values for a maximum FM signal [21]. The modulation frequency was set at 111 MHz, which was found to be the beginning of the white shot noise plateau. At lower frequencies an increase in noise was observed due to the increasing influence of $1/f$ noise (excess noise) contributions, while at higher modulation frequencies the signal decreased because of the lower detector frequency response.

The absorption cell was filled with NO_2 and its optical density was determined directly to be 5.5×10^{-3}. The corresponding FM signal is shown in Fig. 4 and it has a peak to peak value of 13.3 V. The noise was recorded with the current ramp turned off and it is shown with an expanded y scale in the upper right hand corner of Fig. 4. The rms noise value was calculated independently from the digitized signal and determined by a lock-in amplifier (Ithaco 399) with analog noise option. The two determinations agreed to within 5%. With rms noise of 64 mV, a signal to noise ratio of 208 was achieved at a low pass filter bandwidth of 200 kHz. The achieved SNR corresponded to the detectable optical density of 2.65×10^{-5}. By inserting a neutral density (ND 0.33) filter in the optical path, the measured rms noise decreased by about 3 dB, indicating that the performance of the instrument was indeed "quantum limited" [9]. This method can be used as a fast and effective test of "quantum limited" performance. In the case of sensitivity limitations due to low frequency noise, a noise reduction of about 6 dB can be expected.

Without changing the experimental parameters, the absorption cell was evacuated until a signal to noise ratio of 4 was achieved. The FM spectra obtained during the evacuation are shown in Fig. 5. The NO_2 pressure was then kept constant at a value corresponding to an optical density of 1.1×10^{-4}, and the FM spectra were averaged to improve the SNR. Figure 6 shows a single spectrum and the spectra obtained by averaging 32 and 128 spectra. By averaging 128 spectra, the SNR improved to 44 at the original optical density of 1.1×10^{-4}. That corresponds to a detectable optical density of 2.5×10^{-6} at a SNR of 1 and an effective detection bandwidth of 1.56 kHz. It is worth noting that no etalon or other structure is visible in the averaged spectra that could interfere with any sensitiv-

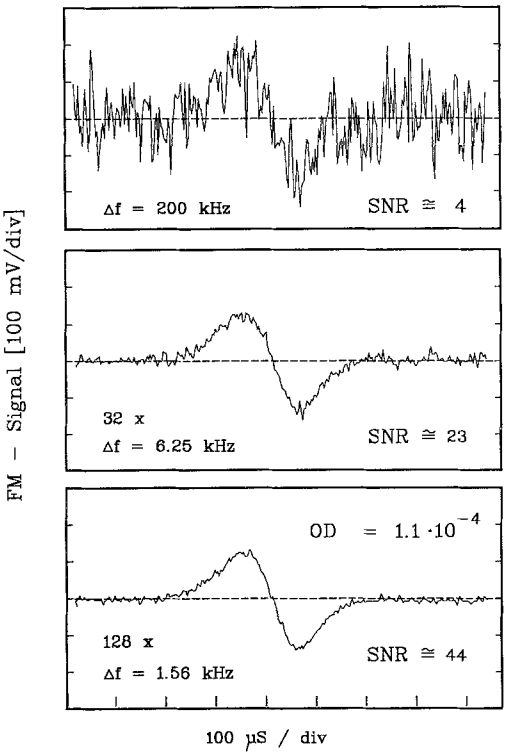

Fig. 6. Demonstration of bandwidth reduction using digital averaging at constant sample gas concentration

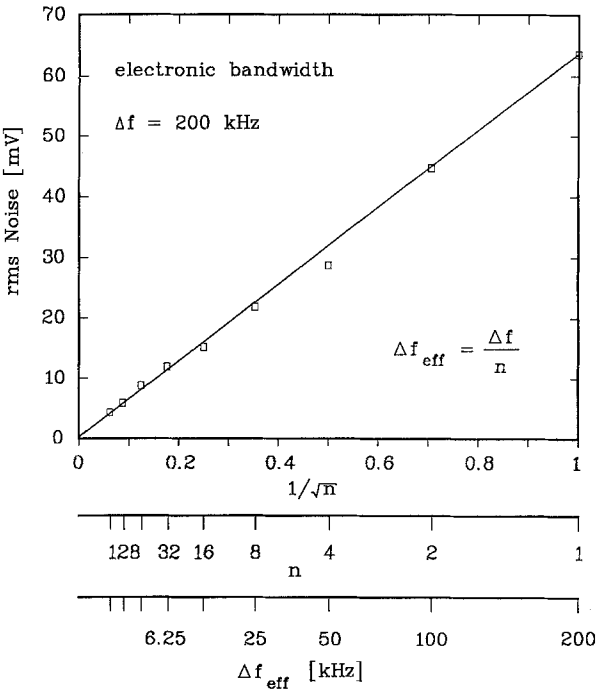

Fig. 7. Comparison of measured noise values with the expected $1/\sqrt{\Delta f}$ dependence (straight line) on the effective detection bandwidth

ity gains by further averaging. Further bandwidth reduction was not within the scope of this experiment. However, Fig. 6 indicates that an optical density of 10^{-6} may be detectable by further averaging.

The noise amplitude should be inversely proportional to the square root of the number of averaged spectra, n, if the noise is caused by random fluctuations of photons or charge carriers. In Fig. 7 the experimental rms noise values are shown as a function of the square root of the number of averaged spectra or, as a function of the effective detection bandwidth, Δf. The experimental values strictly follow the $\sqrt{\Delta f}$ relationship in the effective bandwidth range from 200 to 1.56 kHz. Extrapolating this relationship to the commonly used bandwidth of 1 Hz, the ultimate sensitivity of our FM absorption spectrometer would correspond to:

$$\text{Det. Lim.}_{\text{meas}} = \alpha/(\text{SNR}_{\text{meas}}\sqrt{\Delta f}) = 5.9 \times 10^{-8}. \quad (10)$$

It is at present not clear whether this ultimate detection limit can be achieved solely by further spectra averaging. With the sensitivity increased by another order of magnitude interfering structures such as etalon fringes may appear which are not visible at the 10^{-6} level but which may dominate the averaged spectrum at the 10^{-7} level [22]. On the other hand means are available to cope with interfering etalon fringes [22, 23] and, consequently, optical densities below 10^{-6} should be detectable in practice.

3. Sensitivity Calculation

In this section the measured detection limit of our FM absorption spectrometer will be compared with a calculated "quantum limited" detection limit.

Under proper phase adjustment for the zero baseline component $D(\beta, M, \pi/2)$, the quadrature component of (6) gives an expression for the photocurrent $i(t)$ generated by the incident light with wavelength λ and power P_0 upon a photodetector with quantum efficiency η:

$$i(t) = i_0 D(\beta, M, \pi/2) \cos\omega_{\text{rf}} t, \quad (11)$$

$$i_0 = (e\eta\lambda/hc)P_0, \quad (11a)$$

where e is the electron charge, h Plancks constant, and c the speed of light. Combining (11) and (11a), and calculating the resulting signal power yields:

$$i_S^2 = \tfrac{1}{2} e^2 \eta^2 (P_0 \lambda/hc)^2 D(\beta, M, \pi/2)^2. \quad (12)$$

The noise power under "quantum limited" conditions is dominated by the shot noise term [9] but with the available incident power the thermal noise

contribution, though smaller, has also to be taken into account:

$$i_N^2 = 2e^2\eta(P_0\lambda/hc)\Delta f + 4kT/R_{\text{eff}}\Delta f, \quad (13)$$

where k is Boltzmans constant, R_{eff} the effective noise resistance at temperature T, and Δf the system detection bandwidth.

The mean signal current and the rms noise current were calculated from the parameters listed in Table 2. Most of the parameters were measured. The detector quantum efficiency and the preamplifier noise figure were taken from the manufacturers' specifications. The detection bandwidth was adjusted by an electronic filter (Krohn Hite). The calculated mean signal current is 7.5×10^{-6} A and the rms noise current is 2×10^{-8} A, resulting in a signal to noise ratio at the input of the first amplifier, SNR_{rti}, of 375. Due to the amplifier noise figure, F, of 1.7 in the 50 Ohm system the calculated signal to noise ratio degrades at the low pass filtered PMPA output of the detection system to $\text{SNR}_{\text{rto}} = 220$ with an error of about 3% due to error propagation. The calculated SNR is in good agreement with the measured SNR value of 208 with an estimated error of 3%. The predicted detectable optical density is then:

$$\text{Det.Lim.}_{\text{calc}} = \alpha/(\text{SNR}_{\text{calc}}\sqrt{\Delta f}) = 5.6 \times 10^{-8} \quad (17)$$

at SNR of 1 and an effective detection bandwidth of 1 Hz. The calculated signal voltage is 18.7 V and the rms noise voltage is 85 mV. The measured signal voltage (13.3 V) and noise (64 mV) are about 30% below the calculated values, which is caused by impedance mismatch in the detector-preamplifier combination.

Although the measured and calculated SNR differ by only 6%, a few additional refinements could further improve the agreement. Photovoltaic detectors have to be biased to achieve a high frequency response which is necessary for FM technique, however, the p-n junction when biased is known to generate additional shot noise and this should be taken into account. Although the modulation frequency of 111 MHz was far from the −3 dB cutoff frequency of the detector at 200 MHz, the detector signal is still slightly attenuated. Added corrections for bias noise, detector frequency response and thermal detector noise all increase the calculated noise and so reduce further the calculated SNR value.

Table 2. Set of parameters used for sensitivity calculations

η = 67%	Detector quantum efficiency
P_0 = 1450 μW	Measured laser power on detector
λ = 6.25 μm	Measured laser wavelength
$\Delta\delta = \alpha L/2 = 0.0025$	Measured absorption
β = 1.1	Measured FM modulation index
Δf = 200 kHz	Detection bandwidth
T = 298 K	Preamplifier temperature
R = 180 Ohm	Preamplifier input resistance
F = 4.6 dB	Preamplifier noise figure
G = 94 dB	Measured overall amplifier gain

4. Discussion

The results of this work are summarized in Fig. 8 in terms of detectable optical density at a given detection bandwidth. The lower line represents the calculated optical density detectable by our FM absorption spectrometer, and its theoretically expected $\sqrt{\Delta f}$ dependence on the effective detection bandwidth. The line was constructed from the calculated detection limit of 5.6×10^{-8} with SNR of 1 at 1 Hz detection bandwidth and a laser power of 1450 μW. The validity of the theoretical noise versus bandwidth relationship was verified between 200 and 1.56 kHz. The optical densities of NO_2 measured during the cell evacuation are represented by the circles on the vertical line. The numbers in brackets show the measured SNR of the individual FM absorption spectra. Further evacuation of the absorption cell would yield a FM spectrum with SNR of 1 corresponding to a detectable optical density of 2.7×10^{-5} at a detection bandwidth of 200 kHz. This values represented by a full circle on the calculated line (SNR = 1, P = 1450 μW), showing that the cell evacu-

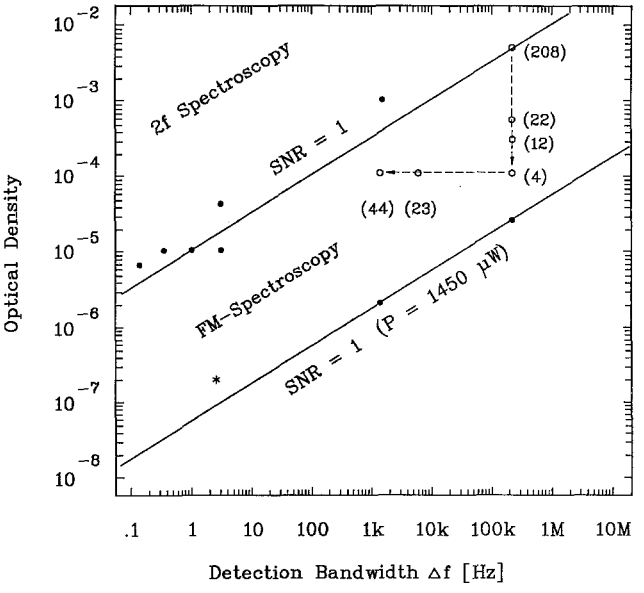

Fig. 8. Spectroscopic map of minimum detectable optical density versus detection bandwidth. The values in brackets are the signal to noise ratios of the measurements from Figs. 5 and 6. The lines of constant SNR correspond to the detection limit of conventional low frequency TDLAS and to the calculated "quantum limited" optical density detectable by our FM system

ation is in excellent agreement with the calculated "quantum limited" sensitivity. The points connected by the horizontal line represent the improvement in SNR achieved by averaging an increasing number of individual spectra with an optical density of 1.1×10^{-4}. Evacuation of the absorption cell would give averaged FM spectra with a SNR of 1 at an effective detection bandwidth of 1.56 kHz corresponding to a detectable optical density of 2.5×10^{-6}. This demonstrated performance is denoted by a full circle. The absence of any etalon structure in the averaged spectra indicates that optical densities of 1×10^{-6} and below may be readily detectable.

Recently, Cooper and Carlisle [22] achieved the near "quantum limited" FM-TDLAS performance when measuring absorption spectra of NO in a 15 cm long absorption cell. They reported a detection limit (SNR = 1) of 1.8×10^{-7} and 2.4×10^{-7} with a 2.44 Hz detection bandwidth by a single and two tone FM technique, respectively. Although the two tone FM technique was expected to perform better than the single tone [17, 21], the difference between the performance of both techniques was marginal in respect to the improvements compared with the conventional TDLAS techniques. The performance reported by Cooper and Carlisle [22] is indicated by an asterisk in the left lower corner of Fig. 8. Taking the lower power of their laser into acount (650 μW), their data agree well with the performance of our FM-TDLAS. It is worth mentioning that despite the use of off-axis paraboloid mirrors, we observed no pronounced etalons at the 1×10^{-5} level of optical density in our instrument. Optical fringes at this level prompted Cooper and Carlisle [22] to use additional signal filtering.

The FM results of Cooper [22] agree excellently with the extrapolation of our data to lower effective detection bandwidths. It is worth noting that similar results were obtained with diode lasers from a different manufacturer. This similarity indicates that the recently reported frequency dependence of the laser noise [9] may be universally applicable to all single mode lead-salt diode lasers.

In the upper left hand corner of Fig. 8 the performance of several TDLAS instruments of conventional design are represented. The data are taken from Table 1 and the points can be connected roughly by a straight line which shows the theoretical bandwidth dependence. Our experimental points show clearly that by the implementation of the FM technique, the TDLAS detection limits can be improved by approximately two orders of magnitude, at least at effective detection bandwidths above 1 kHz. The improvement in the detection limits by two orders of magnitude is in excellent agreement with the expected noise reduction of 40 dB when applying high instead of low frequency modulation [9]. It is also consistent with the results reported by Cooper and Carlisle [22].

5. Conclusions

The results of this work and the work of Cooper and Carlisle [22] indicate that, by implementation of the FM technique, the detectable optical density of the TDLAS instruments can be improved by approximately two orders of magnitude at a given detection bandwidth. So far the capabilities of the FM technique have been demonstrated only with a short absorption cell instead of the multiple reflection cell commonly used in high sensitivity trace gas TDLAS monitors. In practical terms, the demonstrated improvement means that FM-TDLAS instruments can achieve the same trace gas detection limits with a single pass instead of multipass cell leading to a simpler and more rugged optical setup. The introduction of the FM technique could stimulate the development of cheaper TDLAS monitoring instruments.

According to Fig. 8, the same optical density can be detected about 10^4 faster by the FM technique than by the conventional TDLAS techniques. In practical terms the implementation of the FM technique enables trace gas measurements to be made with a frequency far greater than 10 Hz. The practical measuring speed of the TDLAS instrument will then be limited by the exchange of the air in the absorption cell. By minimizing the cell volume, and maximizing the sample flow the gas exchange frequency could possibly be enhanced to 1–10 Hz. Such fast measurements will be very useful for airborne applications and they are a prerequisite of flux measurements by eddy-correlation technique [24].

However, for monitoring of trace gases at even lower mixing ratios than have been measured before, the use of multiple reflection cells will remain indispensable. In this case the sensitivity improvement by the FM technique will be partly offset by the attenuation of the laser power due to reflective losses in such cells. The multiple reflection cells can additionally degrade the FM-TDLAS performance by formation of etalons [1]. The improvement of the TDLAS detection limits that can be achieved practically with multiple reflection cells is now being investigated in this laboratory.

Acknowledgements. We would like to thank M. Tacke from the Fraunhofer Institute for Metrology in Freiburg, FRG, for providing the first specimens of a newly developed MBE laser for these measurements. The help of D. Haaks from Spectra Physics who modified the laser control module to reduce its noise is also gratefully acknowledged. This work has been funded by the German Ministry of Research and Technology (BMFT).

References

1. D.R. Hastie, G.I. Mackay, T. Iguchi, B.A. Ridley, H.I. Schiff: Environ. Sci. Technol. **17**, 352A (1983)
2. R. Grisar, H. Preier, G. Schmidtke, G. Restelli (eds.): *Monitoring of Gaseous Pollutants by Tunable Diode Lasers* (Reidel, Dordrecht 1987)
3. C.R. Webster, R.T. Menzies, E.D. Hinkley: In *Laser Remote Chemical Analysis* ed. by R.M. Measures (Wiley, New York 1988) p. 163
4. D.T. Cassidy, J. Reid: Appl. Opt. **21**, 2527 (1982)
5. J.A. Silver, A.C. Stanton: Appl. Opt. **26**, 2558 (1987)
6. G.W. Sachse, G.F. Hill, L.O. Wade, M.G. Perry: J. Geophys. Res. **92**, 2071 (1987)
7. A. Fried, R. Sams, W.W. Berg: Tunable Diode Laser Development and Spectroscopy Applications (Proceedings of SPIE, Volume 438, W. Lo editor, Washington 1983)
8. J. Reid, M. El-Sherbiny, B.K. Garside, E.A. Ballik: Appl. Opt. **19**, 3349 (1980)
9. P. Werle, F. Slemr, M. Gehrtz, C. Bräuchle: Appl. Opt. (1989) (in press)
10. J.L. Hall, T. Baer, L. Hallberg, H.G. Robinson: In *Laser Spectroscopy* V, ed. by A.R.W. McKellar, T. Oka, B.P. Stoicheff, Springer Ser. Opt. Sci. Vol. **30** (Springer, Berlin, Heidelberg 1981) p. 16
11. G.C. Bjorklund: Opt. Lett. **5**, 15 (1980)
12. W. Lenth: Opt. Lett. **8**, 575 (1983)
13. W. Lenth: IEEE J. QE-**20**, 1045 (1984)
14. M. Gehrtz, W. Lenth, A.T. Young, H.S. Johnston: Opt. Lett. **11**, 132 (1986)
15. G.C. Bjorklund, M.D. Levenson, W. Lenth, C. Ortiz: Appl. Phys. B **32**, 154 (1983)
16. M. Osinsky, J. Buus: IEEE J. QE-**23**, 9 (1987)
17. D.E. Cooper, R.E. Warren: Appl. Opt. **26**, 3726 (1987)
18. S. Kobayashi, Y. Yamamoto, M. Ito, T. Kimura: IEEE J. QE-**18**, 582 (1982)
19. W. Lenth, M. Gehrtz: Appl. Phys. Lett. **47**, 1263 (1985)
20. J.A. Silver, A.C. Stanton: Appl. Opt. **27**, 4438 (1988)
21. N.-Y. Chou, G.W. Sachse: Appl. Opt. **26**, 3584 (1987)
22. D.E. Cooper, C.B. Carlisle: Opt. Lett. **13**, 719 (1988)
23. C.R. Webster: J. Opt. Soc. Am. B **2**, 1464 (1985)
24. B.B. Hicks, M.L. Wesely, J.L. Durham: Critique of methods to measure dry deposition: Workshop summary EPA-600/9-80-050, Washington DC, EPA, 83, 1980